INTERANNUAL VARIABILITY OF THE CALIFORNIA CURRENT—PHYSICAL FACTORS

DUDLEY B. CHELTON
Jet Propulsion Laboratory
California Institute of Technology
Pasadena, CA 91103

ABSTRACT

Monthly variations in the physical characteristics of the California Current system from 1950 to 1979 are examined to explore the potential causes of zooplankton variability. It is shown that variations in the large-scale zooplankton biomass cannot be explained solely on the basis of coastal upwelling. However, large-scale advection in the California Current appears to play a major role in controlling the large-scale zooplankton variability over interannual time scales. Coastal tide gauge records provide a simple and convenient means of monitoring this interannual variability, and since these records date back to the early 1900's, they provide a very long record of large-scale, low-frequency changes in the California Current.

An attempt is made to identify the source of these large-scale changes in the flow. It is shown that, in many cases, the variations bear a strong resemblance to El Niño events in the eastern tropical Pacific with a time lag of several months. There are occasionally, however, strong events off the coast of California with no eastern tropical Pacific counterpart. Particular attention is focused here on a strong event during 1978 where anomalous poleward flow of the California Current was associated with an expected increase in water temperature but an unexplainable decrease in salinity.

RESUMEN

Se examinan las variaciones mensuales en las características físicas del sistema de la Corriente de California de 1950 a 1979, para explorar las causas potenciales de la variabilidad del zooplancton. Se muestra que las variaciones en la biomasa del zooplancton de gran escala no se pueden explicar solamente a base de la surgencia costera. Sin embargo, la advección de gran escala en la Corriente de California parece jugar un papel importante en el control de la variabilidad del zooplancton de gran escala a través de escalas de tiempo interanuales. Los registros de mareómetros en la costa permiten un método fácil y conveniente de seguir esta variabilidad interanual, y ya que estos registros datan del comienzo de los años 1900, proveen una documentación que cubre un largo período de cambios de gran escala y de baja frecuencia en la Corriente de California.

Se intenta identificar el origen de estos cambios de gran escala en el flujo. Se ha mostrado que, en muchos casos, las variaciones son muy parecidas a los acontecimientos de El Niño en el Pacífico oriental tropical, con un retraso de varios meses. Sin embargo, se encuentran en ocasión unos fuertes acontecimientos frente a la costa de California, sin la ocurrencia de su contraparte en el Pacífico oriental tropical. En este trabajo se enfoca en un acontecimiento fuerte durante 1978, donde el flujo anómalo de la Corriente de California hacia el polo estuvo asociado con el aumento que se esperaba en la temperatura del agua, pero con un descenso inexplicable en la salinidad.

INTRODUCTION

The California Cooperative Oceanic Fisheries Investigation (CalCOFI), as it was initiated by Sverdrup and others in the late 1940's, was primarily intended as an ecological study of the fisheries off California. Numerous studies have noted that high biomass in the California Current is associated with low water temperature (Reid et al. 1958; Colebrook 1977). It is generally believed that the source of the cold water is coastal upwelling driven by the longshore component of local wind stress. The wind-driven offshore Ekman transport results in a divergence of water at the coast which must be replaced by the cold, nutrient-rich water at depth. Analyzing 21 years of CalCOFI zooplankton data (1949-69), Bernal (1980) and Bernal and McGowan (1981) have suggested an alternative mechanism for large-scale biological changes. They have presented evidence that advection of nutrient-rich water from high latitudes plays a major role in controlling the biomass of the eastern Pacific Ocean. This importance of advection to zooplankton variability in the California Current was first suggested by Wickett (1967).

In addition to zooplankton measurements, vertical profiles of temperature and salinity have been routinely made by CalCOFI. These hydrographic surveys have continued through 1979 on a fixed grid system providing a 30-year record of the physical characteristics of the California Current. The purpose of this study is to examine these time series of temperature and salinity and their relation to the large-scale biological changes described by Bernal (1979; 1980). The vertical hydrographic profiles can be used to
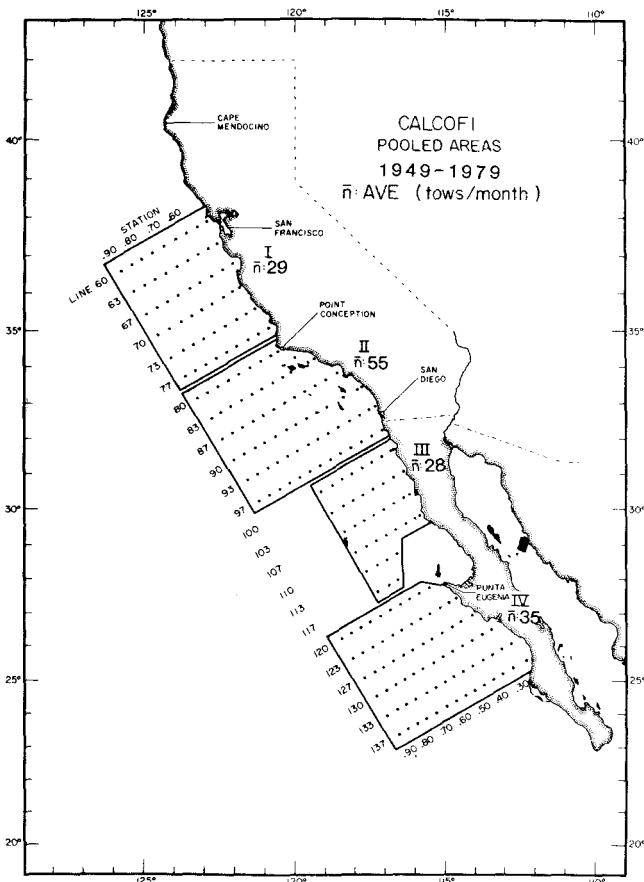
Figure 1. The four regions in the California Current over which spatial averages of zooplankton volume were computed: n̄ refers to the average number of individual samples pooled into a typical monthly estimate.
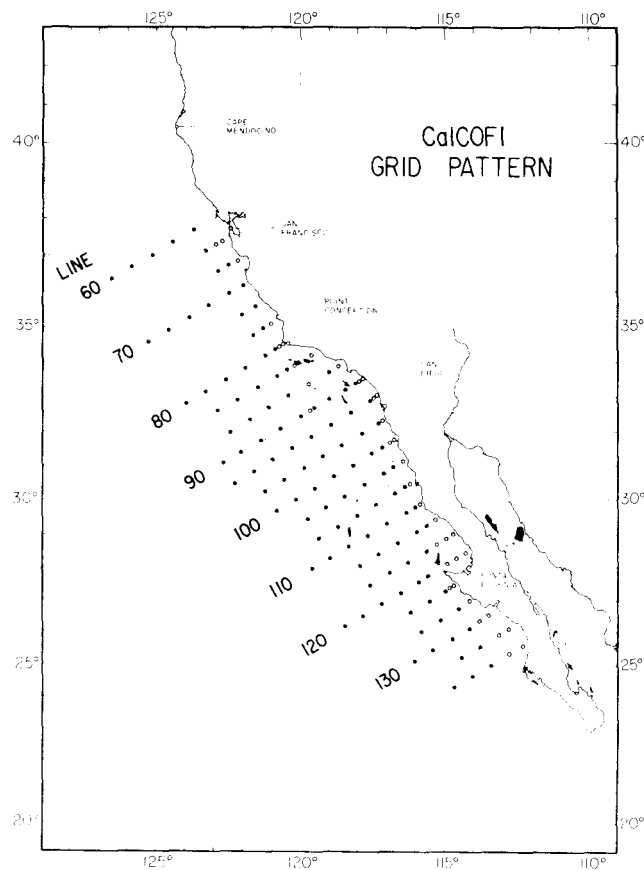

Figure 2. Grid of CalCOFI hydrographic stations occupied 40 or more times over the 30-year time period from 1950 to 1979. CalCOFI cardinal lines are labeled.

compute the steric height of the sea surface from which relative geostrophic flow can be inferred. This allows a quantitative assessment of the relation between advection and zooplankton biomass in the California Current.

DATA DESCRIPTION

Time series of log-transformed zooplankton volume from 1949 to 1979 were obtained from P. Bernal for the four regions of the California Current shown in Figure 1. Monthly means were constructed by averaging all observations at stations within each geographical area for each calendar month. The details of this procedure can be found in Bernal (1979; 1980).

The CalCOFI hydrographic (temperature and salinity) data were obtained from Larry Eber at the National Marine Fisheries Service in La Jolla, California. Monthly mean values from 1950 to 1979 were interpolated to 16 standard depths down to 1000 m. The data were then sorted by spatial grid location, and those with fewer than 40 observations over the 30-year time period were rejected from the analysis that fol-

lows. The number of spatial grid points remaining amounted to a total of 150 of which 114 extend to a depth of 500 m or more (Figure 2). The typical number of observations at any given grid point over the 30-year period was around 90.

SEASONAL VARIABILITY

The first analysis step was to describe the seasonal variability of zooplankton biomass. The method used consists of computing the 30-year algebraic mean value for each month of the year. The resulting mean annual cycles for each of the four areas are shown in Figure 3. The zooplankton biomass is largest at high latitudes and decreases equatorward. A seasonal signal is clearly present in each of the areas with a maximum generally occurring in late spring or early summer and a minimum in early winter. The maximum and minimum in Area IV occur about two months later than in those areas further north.

The annual cycles of the equatorward longshore component of wind stress for each of the four areas are also shown in Figure 3. These winds may be consid-
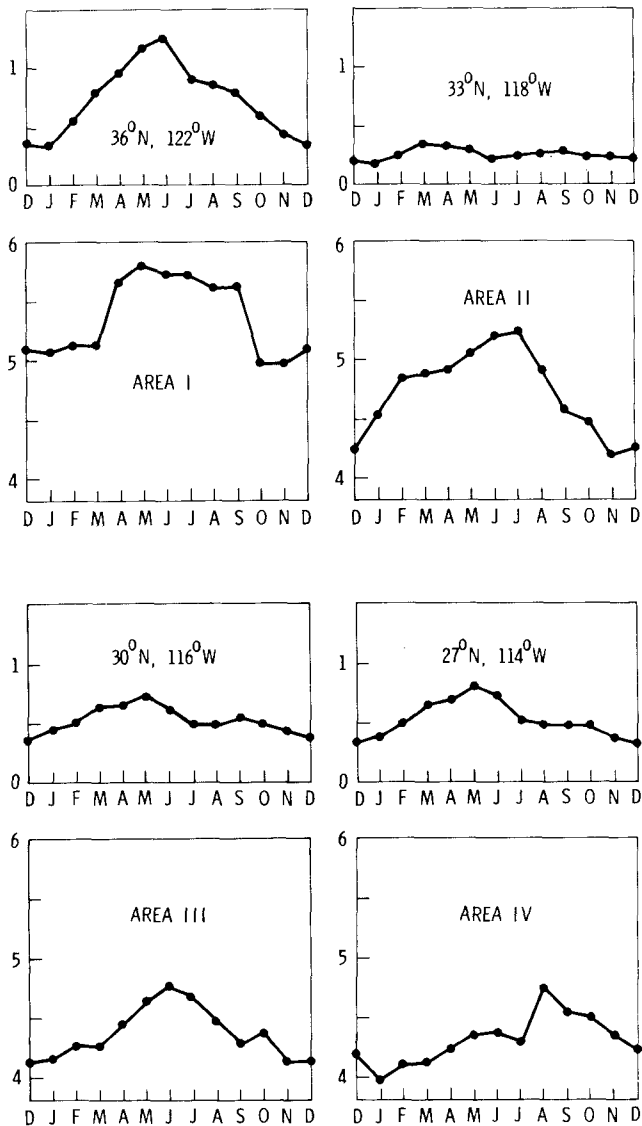
Figure 3. Annual cycles of the longshore (equatorward) component of wind stress in dynes/cm² (upper panels) and the zooplankton volume in log$_e$ [ml/1000 m³] (lower panels) for each of the four geographical regions shown in Figure 1.

ered an index of coastal upwelling intensity: an increase in equatorward longshore winds corresponds to an increase in coastal upwelling. The seasonal mean wind stress values were taken from Nelson (1977) who compiled direct ship observations by 1-degree square areas from records dating back to the mid-19th century. These are probably the best available long-term measure of winds over the California Current. The figure shows that the winds are favorable for coastal upwelling year-round in each of the four areas with a maximum intensity in late spring or early summer.

A comparison of winds and zooplankton variability in Area III reveals what appears to be a strong relation between the two. There are two peak upwelling

periods. The strongest occurs in May, and it is followed one month later by a maximum in zooplankton volume. There is a secondary peak upwelling period in September, again followed one month later by a peak in zooplankton volume. From this simple relation, it is tempting to conclude that coastal upwelling is the primary source of nutrients controlling zooplankton biomass in the California Current. However, this appealing picture breaks down in the other three areas where there appears to be little or no relation between coastal upwelling (as indexed by the longshore wind stress) and zooplankton biomass.

It might be argued that the mean seasonal cycle has not been properly resolved here. This seems unlikely in the case of the wind data but could possibly be true in the case of the somewhat more limited zooplankton data set. There are other methods for defining the seasonal cycle, but considering the large number of zooplankton observations involved, it is doubtful that the resulting time series would differ significantly from those shown in Figure 3. An alternative explanation for the poor agreement with coastal upwelling is that some other process is at least partially responsible for controlling the zooplankton variability.

Wickett (1967) found a significant relation between zooplankton volume off California and wind forcing in the Alaskan Gyre one year earlier. He has suggested that the zooplankton off southern California respond to the upwelled nutrients in the Alaskan Gyre that are advected downstream by the southward flowing California Current. Bernal (1980) and Bernal and McGowan (1981) have also presented evidence from 21 years of data that advection plays a major role in controlling the zooplankton biomass. They found a significant correlation between zooplankton variability and the transport of low-salinity water across CalCOFI line 80 (running directly offshore from Point Conception). The objective of this study is to examine the importance of large-scale advection to zooplankton biomass in greater detail using the complete 30-year CalCOFI zooplankton and hydrographic data sets (1950-79).

The problem with looking at cause and effect relationships in the seasonal cycle is that nearly all geophysical and biological time series show a seasonal variation and any two seasonal cycles are highly correlated if one allows for a phase lag. However, since there are only 12 (nonindependent) data values, the statistical significance of any relation is based on a very small number of degrees of freedom. It is therefore better to remove the annual cycle from the data and look for causality in the residuals. The remainder of this study deals only with nonseasonal aspects of variability.

NONSEASONAL VARIABILITY

Anomalous zooplankton volume for a given month is defined to be the departure of the observed value from the seasonal mean value as shown in Figure 3 for that particular month. After removing the seasonal cycle, the log-transformed zooplankton anomalies for each of the four regions were normalized to have unit standard deviation. The resulting time series for 1949 to 1969 are shown in Bernal (1979). It is apparent from these figures that, underlying the seasonal signal, there are large year-to-year variations in the zooplankton biomass which tend to persist for 1-3 years. This anomalous behavior is in many respects more interesting than the seasonal variability discussed in the last section. In this study, Bernal's time series of nonseasonal zooplankton volume have been extended through 1979.

The wind-stress data were seasonally corrected in the same manner. The temporal and spatial sampling distribution of the direct ship observations compiled by Nelson (1977) is adequate for describing the seasonal variability discussed in the last section but not sufficient to resolve the detailed anomalous year-to-year variability of interest here. Instead, geostrophically computed winds produced by Fleet Numerical Oceanography Center (FNOC) were used to derive time series of wind-stress anomalies from each of the four areas. A detailed explanation of the method used by FNOC in computing these winds can be found in Caton et al. (1978).

The time-lagged correlation between nonseasonal zooplankton volume and the local equatorward longshore component of wind stress is shown in Figure 4 for each of the four areas. The results clearly indicate that locally forced coastal upwelling is not the dominant process controlling the zooplankton biomass. Zooplankton volume does tend to be positively correlated with upwelling, but the relationship is at best very weak.

From the individual time-series plots of zooplankton volume shown in Bernal (1979), it is evident that the nonseasonal variations in all four areas are very closely related. This study focuses attention on only the very large-scale variability which can be extracted by averaging the four individual time series. The resulting index of large-scale secondary productivity in the California Current is shown in Figure 5a. The figure reveals a strong interannual signal.

The cause of these significant variations in zooplankton biomass can be investigated by examining the nonseasonal variability of temperature and salinity in the California Current. The sampling distribution of the hydrographic data at each of the individual stations shown in Figure 2 is not adequate to accurately resolve
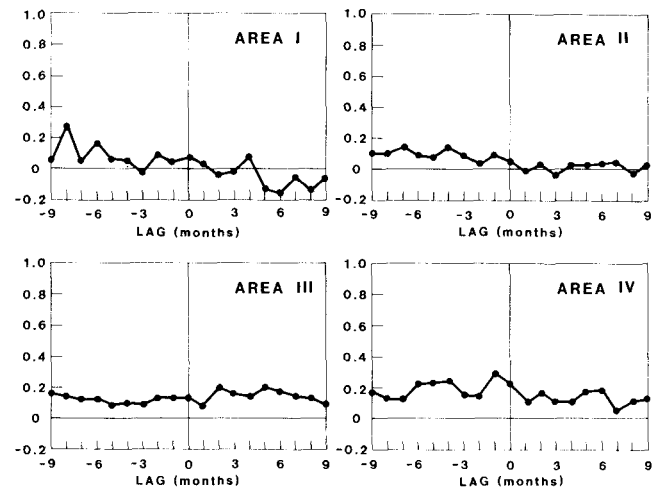

Figure 4. Correlation between nonseasonal zooplankton volume in month t and the local longshore (equatorward) component of wind stress in month $(t+\text{lag})$ for each of the four geographical regions in Figure 1.

the seasonal cycle by the long-term averaging method used on the zooplankton data. In particular, the sampling is biased toward summertime cruises. The statistical reliability of seasonal mean values estimated using the averaging technique varies from month to month and from location to location, depending on the number of samples used to estimate the mean.

An alternative and preferred method is to represent the temperature and salinity seasonal cycles by two harmonics, one with an annual and the other with a semiannual period. These two sinusoids were fit to the full 30 years of CalCOFI hydrographic data using least squares regression analysis. It should be noted that when the number of samples is large and evenly distributed throughout the year, the annual cycle computed using the harmonic method very closely resembles that computed by the averaging technique. The resulting seasonal cycles (described in Chelton, 1980) were used to compute monthly anomalies of temperature and salinity as with the zooplankton data.

Of particular interest here are the very large-scale nonseasonal variations of temperature and salinity. There are a number of methods for extracting the large-scale aspects of a parameter. The simplest is to form spatial averages as was done with the zooplankton data. This technique is obviously of limited value in cases where there are large horizontal variations in the parameter or when the horizontal gradients of the parameter are of primary interest (as in the case of the steric height data to be examined later in this section). All the important information can easily be lost using such a procedure. An alternative method that proves to be extremely useful is a technique called Empirical Orthogonal Function (EOF) or principal component analysis. The method essentially consists
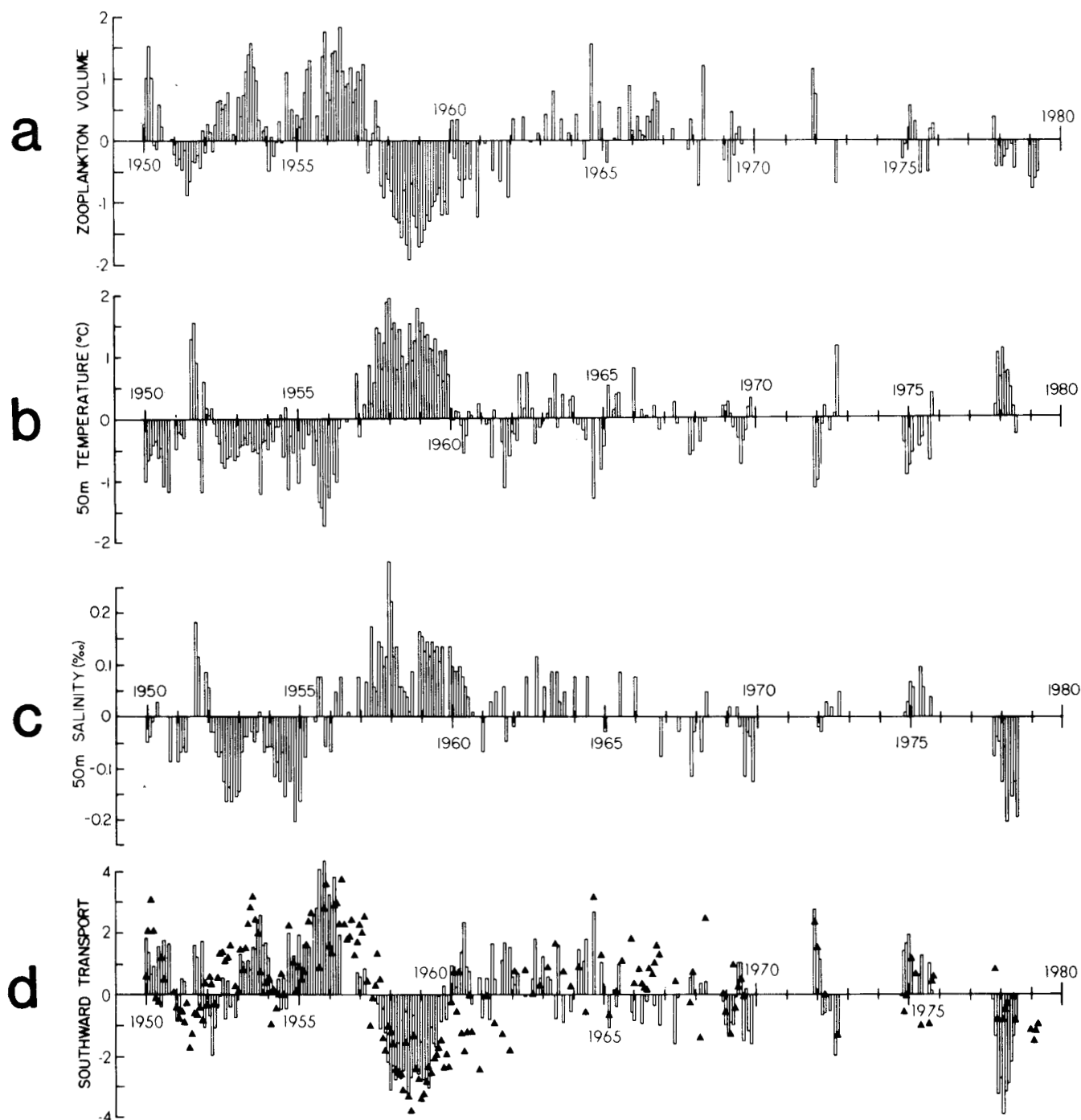
Figure 5. Time series of nonseasonal values of four parameters in the California Current: a) The average of the individual zooplankton time series in the four regions shown in Figure 1; b) The amplitude time series of the principal EOF of 50 m temperature shown in Figure 6; c) The amplitude time series of the principal EOF of 50 m salinity shown in Figure 9; d) The amplitude time series of the principal EOF of 0/500 db steric height shown in Figure 10. The zooplankton time series in a) has been reproduced as the triangles in d).

of separating the time and space dependence of a parameter in a manner that optimally describes the variance in a least squares sense. A time series of maps of some scaler variable $\phi(x,t)$ at N locations x can be expressed in terms of a set of N orthogonal functions $F_n(x)$ by

$$\phi(x,t) = \sum_{n=1}^{N} a_n(t) F_n(x).$$

The EOFs are uniquely defined among all possible sets of orthogonal functions by the constraint that their

time amplitudes a_n (t) be uncorrelated over the data set. A detailed explanation of the method used to compute F_n (x) and $a_n(t)$ can be found in Davis (1976). Methods of filtering to extract the large-scale aspects of variability in gappy data sets such as the CalCOFI hydrographic data are described in Chelton (1980).

The dominant spatial EOF of anomalous water temperature at 50 m depth is shown in Figure 6. Shallower temperature measurements were found to be very noisy. This pattern accounts for nearly half of the variability at 50 m over all 150 stations. It indicates that the temperature generally rises or falls (depending on the sign of the amplitude time series) everywhere over the California Current. The magnitude of temperature changes are largest close to the coast and tend to decay to a value of zero offshore. The time series associated with this pattern of 50 m temperature is shown in Figure 5b. The results are perhaps not surprising: The water temperature bears a very strong inverse relationship to the zooplankton variability. High zooplankton biomass is associated with cold water. Conversely, anomalously warm periods tend to be associated with low zooplankton volume.

There are two processes by which the water in the

California Current can cool: either by upwelling of cold water from depth or by advection of cold water from higher latitudes. Either process provides the nutrients necessary for increased zooplankton productivity. Separating these two effects is a difficult task because the two are closely related. An increase in the flow of the California Current, either nonlocally forced or driven by the local wind stress (upwelling), results in an increased southward advection of cold water. It also results in a geostrophic adjustment of the density field with isotherms tilting in a manner that cools the nearshore waters.

Although both processes produce a similar signature in the temperature field, they differ in their effect on salinity. The mean cross-shore salinity distribution along CalCOFI line 93 is shown in Figure 7. The important features are the same throughout the
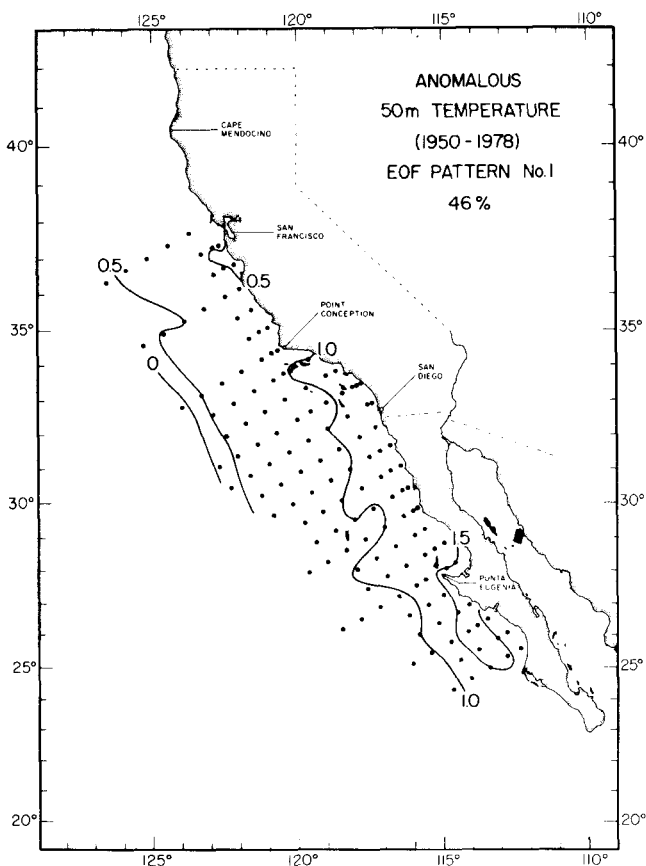

Figure 6. The principal spatial EOF of nonseasonal temperature at 50 m depth. The function values have been normalized to have mean square value of 1.
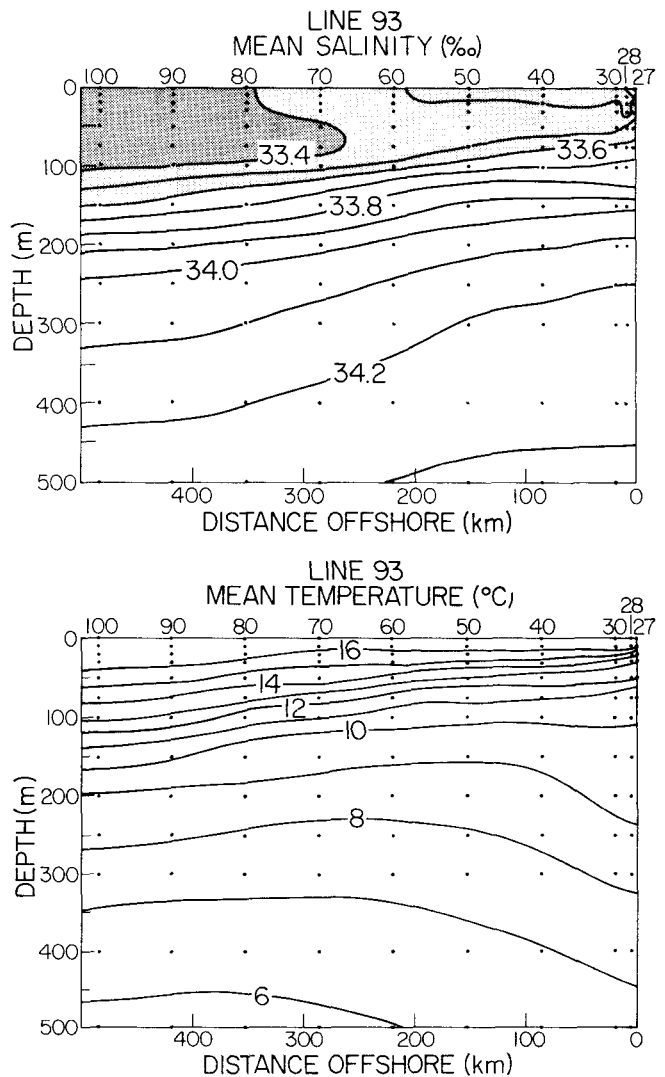

Figure 7. The mean cross-shore salinity and temperature distribution along CalCOFI line 93. Station numbers are shown along the upper axis.

California Current. The salinity increases with depth and decreases offshore. (Farther offshore beyond station 100, the salinity near the surface begins to increase again.) Thus, upwelling would lead to an increase in the nearshore salinity, and conversely, downwelling would tend to decrease the nearshore salinity. Then, if upwelling of deeper water (and nutrients) were solely responsible for fluctuations in secondary productivity, high zooplankton biomass would be associated with high salinity.

Advection produces quite a different signature in the salinity field. A section showing the mean longshore salinity distribution in the California Current is shown in Figure 8. The increase in salinity with depth previously noted in Figure 7 is clearly present throughout the California Current. The important feature here is the tongue of low-salinity water extending from high to low latitudes. Increased southward transport would cause the salinity to decrease and, correspondingly, decreased transport would result in an increase in the salinity. If advection of high-latitude water (and nutrients) were responsible for variations in secondary productivity, high zooplankton biomass would be expected to be associated with low salinity.

Because upwelling and advection produce opposite effects on the salinity distribution, the salinity can be used as a tracer for differentiating between the two processes. As with temperature, salinity observations

close to the surface were found to be quite noisy. The dominant EOF of salinity at 50 m is shown in Figure 9. This pattern accounts for 40% of the variability over all 150 stations. It indicates that the salinity tends to increase or decrease simultaneously everywhere over the California Current. The time series associated with this pattern of salinity variability is shown in Figure 5c. It is somewhat noisier than temperature or zooplankton volume (perhaps to some extent reflecting the complex interrelation between upwelling and advection), but high zooplankton biomass generally tends to be associated with low salinity and conversely. The correlation between the two is -0.53. This relation statistically favors advection as the predominant source of nutrients controlling zooplankton biomass.

It should be pointed out that there are some instances when the advective model does not appear to hold. Although temperature and salinity do generally fluctuate in phase, they are out of phase during 1975 and 1978. The extreme 1978 event where low zooplankton volume was associated with low salinity is an indication that not all low-salinity water is high in nutrients. Although advection appears to be the dominant mechanism, it is apparently not the only source of nutrients controlling zooplankton productivity. This will be discussed in greater detail in the next section.
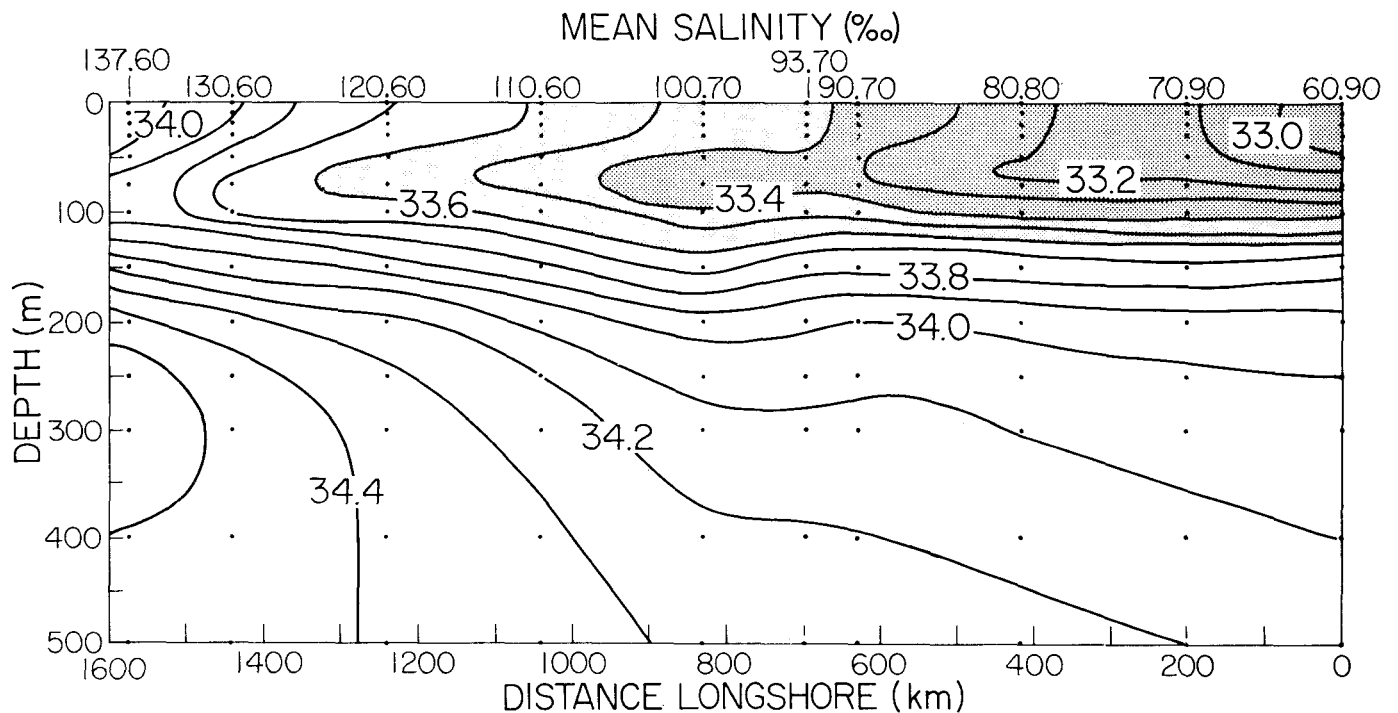
Up until this point, the suggested biological impor-

Figure 8. The mean longshore salinity distribution. The CalCOFI line and station numbers used in the figure are shown along the upper axis. (e.g. 100.70 refers to line 100 station 70).
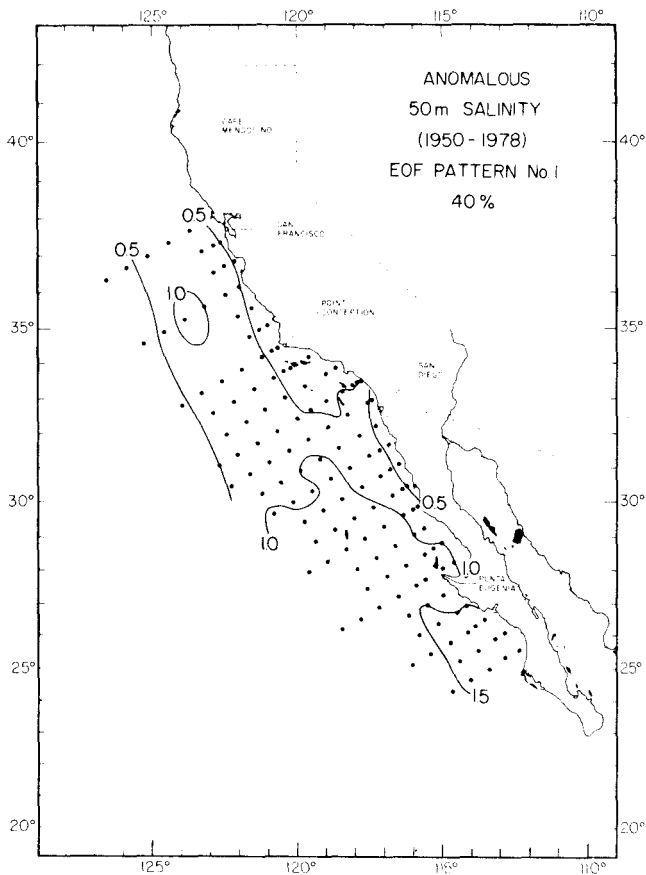
Figure 9. The principal spatial EOF of nonseasonal salinity at 50 m depth. As in Figure 6, the function values have been normalized to have mean square value of 1.
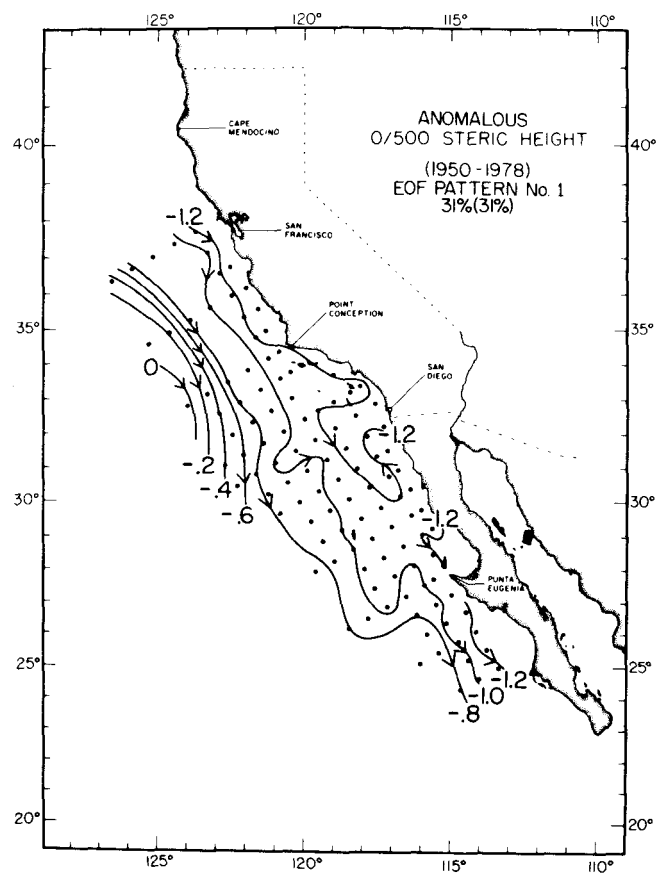

Figure 10. The principal spatial EOF of nonseasonal 0/500 db steric height. As in Figures 6 and 9, the function values have been normalized to have mean square value of 1. Arrows indicate direction of flow when the amplitude time series shown in Figure 5d is positive. Negative values of the time series correspond to a reversal in the anomalous flow (i.e. poleward transport).

tance of advection has been indirect and purely qualitative. The large-scale anomalous variations in the flow of the California Current can be quantified by looking at the steric height, which gives an integrated measure of the effects of temperature and salinity. The steric height of the sea surface relative to a reference pressure surface p_o is computed by

$$h = -\frac{1}{g}\int_{p_o}^{0} \delta \, dp$$

where δ is the specific volume anomaly defined to be departures of the reciprocal value of density from a standard ocean of temperature 0°C and salinity 35⁰/oo. The specific volume anomaly is a function of temperature, salinity, and to a lesser extent pressure. Warm or low-salinity water displaces a larger volume and causes the sea surface to stand higher than cold or high-salinity water. Horizontal gradients of steric height give a measure of the geostrophic flow at the sea surface relative to the reference pressure surface p_o.

The steric height relative to 500 db was computed at

each of the stations shown in Figure 2. The seasonal cycle at each station was then computed and removed in the same manner as for temperature and salinity. The dominant EOF of 0/500 steric height anomalies accounting for one-third of the variability is shown in Figure 10. When the time amplitude of this pattern is positive, the southward flow of the background California Current is intensified. Conversely, when the time amplitude is negative, the southward flow is weakened. A strong enough weakening could actually result in a reversal of the flow.

The time series associated with this pattern of anomalous large-scale advection is shown in Figure 5d where, for easy comparison, the zooplankton time series shown previously in Figure 5a have been reproduced as the triangles. The figure supports the hypothesis that increased southward advection leads to an increase in zooplankton biomass. Correspondingly, when the southward flow is below normal, so is the zooplankton biomass. The time-lagged correlation between the two time series is shown in Figure 11. The plot is distinctly asymmetric and indicates that
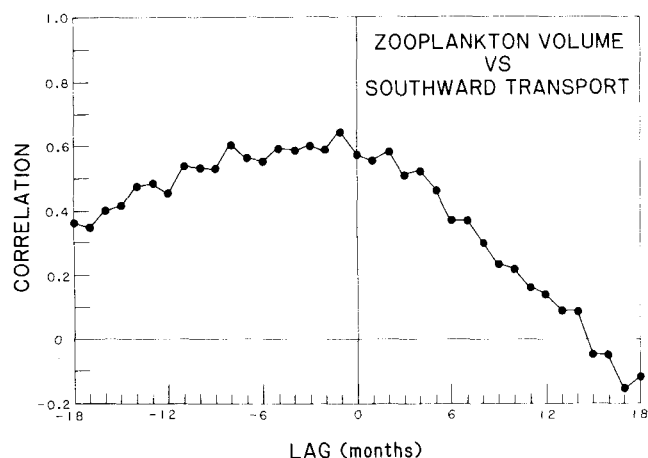
41

Figure 11. Correlation between large-scale zooplankton biomass in month *t* as shown in Figure 5a and anomalous southward transport of the California Current in month (*t*+lag). The index of southward transport is the EOF amplitude time series of 0/500 db steric height shown in Figure 5d.

zooplankton volume is more highly correlated with preceding than with subsequent anomalous flow. That is, the effects of advection on secondary productivity tend to persist for many months. A maximum correlation of 0.65 occurs when advection leads zooplankton biomass by one month. This correlation is rather impressive considering the serious sampling problems associated with both data sets.

It would clearly be advantageous to find a simple means of monitoring these large-scale changes in the flow without taking time-consuming and expensive hydrographic observations from ships. Two potentially useful land-based oceanographic measurements are coastal tide gauge-measured sea level and coastal sea-surface temperature. Figure 12a shows the correlations between sea level and sea-surface temperature at La Jolla and the index of large-scale advection shown in Figure 5d. Both the sea level and sea-surface temperature records have been low pass filtered with a one-year running mean, and the sea level data have been corrected for the inverse barometric effects of atmospheric pressure (1 cm/mb). The results yield further insight into the importance of advection. Both sea level and sea-surface temperature are significantly correlated with anomalous flow; low sea level and cold water are associated with increased southward transport. The interesting feature from Figure 12a is that changes in the flow follow changes in sea level by about one month but *precede* changes in sea-surface temperature by about two months. The lag between changes in flow and changes in sea-surface temperature supports the notion that the source of cold water anomalies in the California Current is advection rather than upwelling.

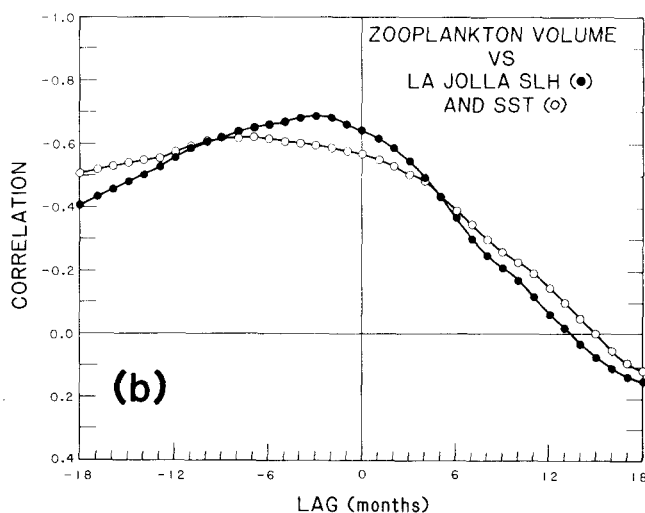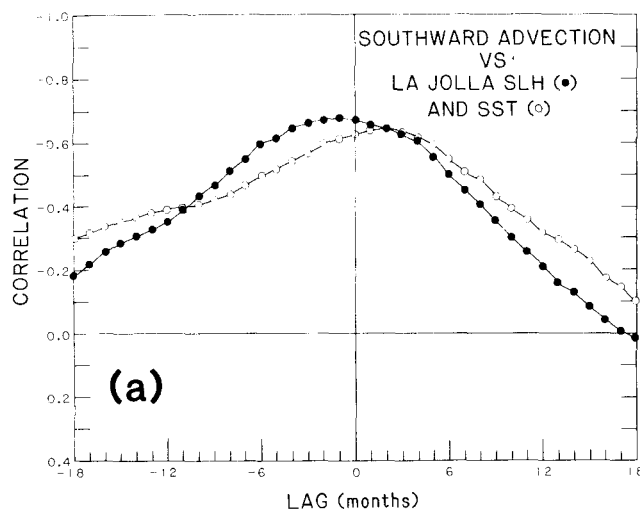The correlations between sea level and sea-surface

Figure 12. Correlations between sea level height (SLH) and sea-surface temperature (SST) in month (*t*+lag) at La Jolla, California, and a) the index of southward advection in month *t* shown in Figure 5d; b) large-scale zooplankton biomass in month *t* as shown in Figure 5a. The sea level data has been corrected for the inverse barometric effects of atmospheric pressure (1 cm/mb).

temperature at La Jolla and the large-scale variability of zooplankton biomass (Figure 5a) are shown in Figure 12b. The sea-surface temperature observations are somewhat noisy, and the zooplankton volume is more closely related to sea level which gives an integrated measure of upper ocean density variations. Sea level anomalies tend to precede changes in zooplankton volume by about three months. Note, however, that the frequencies involved are too low for this to be useful as a predictive tool.

The strong relation between sea level and anomalous flow of the California Current is further demonstrated in Figure 13. The vertical bars represent the index of southward advection shown previously in Figure 5d. The continuous curve represents a one-year running mean of the average of sea level (corrected for
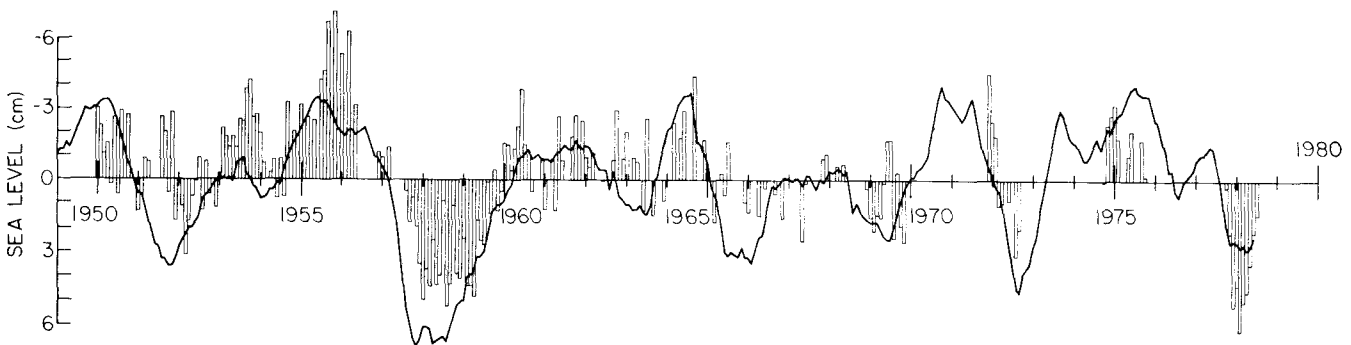
Figure 13. Time series of low-frequency (one-year running mean) sea level (corrected for inverse barometer effects) averaged over San Francisco, Los Angeles, and San Diego. The vertical bars represent the index of southward transport shown previously in Figure 5d. Note that the ordinate for sea level has been inverted; low sea level corresponds to above normal southward flow.

inverse barometric effects) at San Francisco, Los Angeles, and San Diego. Note that the ordinate of sea level has been inverted; low sea level corresponds to above normal southward flow and high sea level signals anomalous poleward flow.

Since tide records date back to the early 1900's, they can give some indication of large-scale changes in the flow of the California Current over the last 80 years. Figure 14 shows the average of sea level at San Francisco, Los Angeles, and San Diego from 1900 to 1979 (again smoothed by a one-year running mean). If these sea level variations can be interpreted as an index of secondary productivity, the figure indicates that very large biological changes occur on a regular basis and tend to persist for time scales of 1-3 years. It would be interesting to compare this time series with the anaerobic sediment records of biological debris described by Soutar (1971).

DISCUSSION

The preceding section has documented a significant interannual variability in both the physical and biological oceanography of the California Current. The results suggest that large-scale variations in zooplankton volume primarily reflect a response to nutrients advected downstream from high latitudes. When the flow weakens, the nutrient input decreases and so does the zooplankton biomass. This zooplankton response to nutrients is presumably indirect, reflecting a response of phytoplankton (the food source of zooplankton) to nutrient availability. The causes of these low-frequency changes in the flow have yet to be identified. Figure 4 indicates that they are apparently not forced by the local wind field.

However, using the sea level records as an index of flow, Figure 15 shows that the strength of the California Current is rather closely related to El Niño occur-
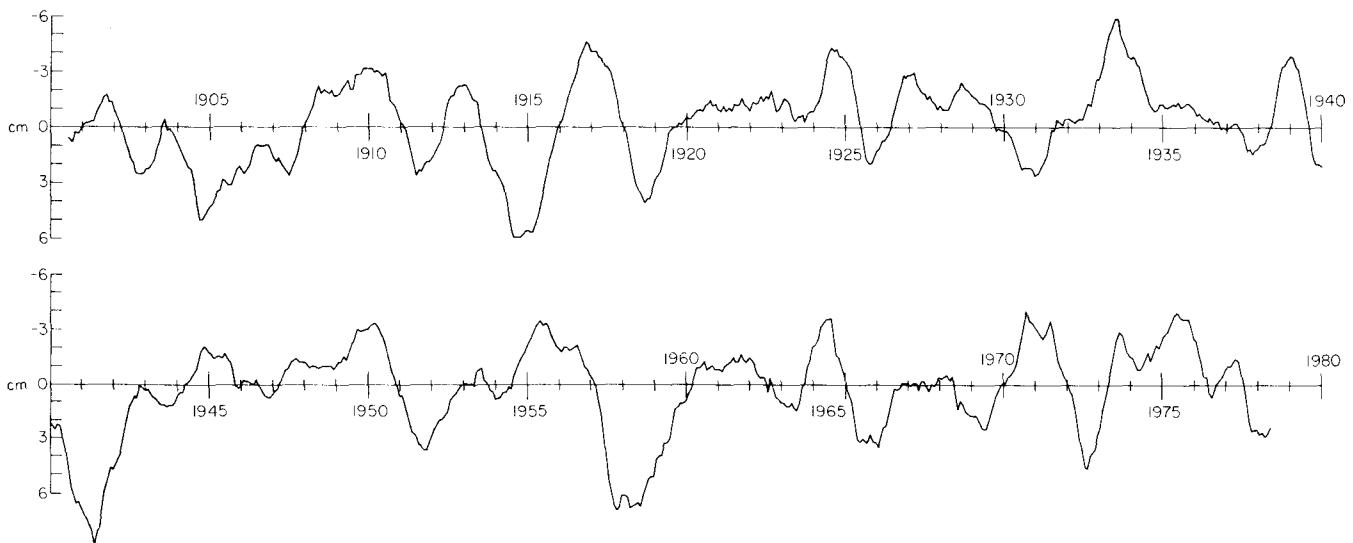

Figure 14. Low-frequency (one-year running mean) sea level averaged over San Francisco, Los Angeles, and San Diego from 1900 to 1979. With some caution, this time series can be taken as an index of large-scale biological changes in the California Current over the last 80 years. Note that the ordinate has been inverted; low sea level corresponds to above normal zooplankton biomass.
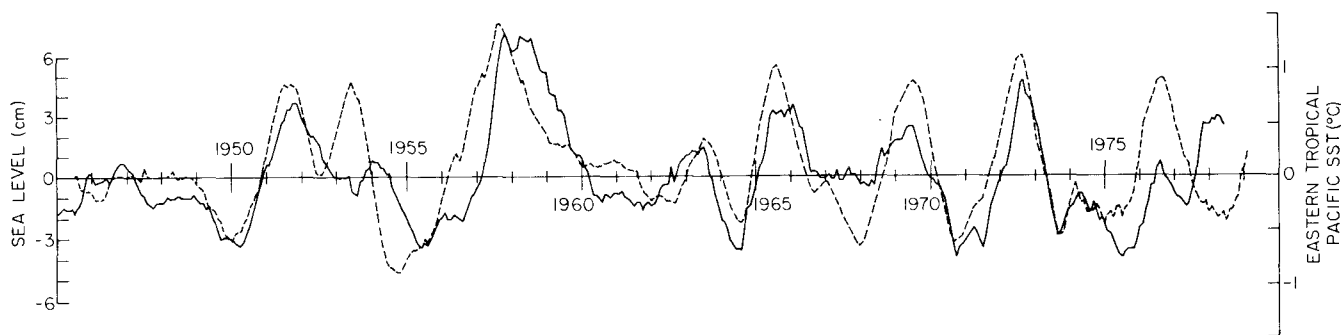
Figure 15. The time series of low-frequency sea level previously shown in Figure 13 (solid line) and low frequency (one-year running mean) sea-surface temperature in the eastern tropical Pacific (dashed line). Note that the sea level ordinate is no longer inverted as in Figures 13 and 14.

rences in the eastern tropical Pacific. The index of El Niño used here (the dashed line) is a one-year running mean of sea-surface temperature averaged over a region in the eastern tropical Pacific from the equator to 10°S and from 80° to 100°W. The major El Niño events of 1957-58, 1965, 1969, and 1972, as well as a number of more minor events are clearly evident in both time series. The correlation between these two time series is 0.72. Note that the ordinate for sea level is no longer inverted as it was in Figures 13 and 14. El Niño is associated with positive California sea level anomalies which (from Figure 13) correspond to anomalous poleward flow.

Figure 15 suggests a tendency for El Niño in the eastern tropical Pacific to lead California sea level by 2-3 months. This lagged relationship can be demonstrated more quantitatively through correlation analysis. Figure 16 is a contour plot of the time-lagged correlation between the El Niño index and low-frequency (one-year running mean) sea level at each of 20 stations from southern Mexico to the tip of the Aleutian Islands. The amount by which sea-surface temperature in the tropics leads sea level along the west coast of North America increases in a fairly systematic manner with increasing distance from the tropics. The El Niño signal in the tropics occurs nearly simultaneously with sea level anomalies at Acapulco but precedes sea level at San Francisco by about three months. The dashed line locates the approximate maximum lagged correlation and corresponds to northward propagation at a phase speed of about 50 cm/sec. This is the character of response expected from simple theoretical considerations which indicate that El Niño originates in that tropics from anomalous forcing by the trade winds. Sea-surface temperature and sea level rise in the eastern tropics, and these sea level anomalies propagate poleward as coastally trapped waves which lead to anomalous poleward geostropic flow (McCreary, 1976).

Although this relation between El Niño and the strength of the flow off California is simple and ap-

pealing, there are several incidences where the relationship breaks down. Most notable are 1953, 1967-68, 1976 and 1978. Special attention will be focused here on the 1978 event when there was anomalous poleward flow (see Figure 13) which would be expected to occur during an El Niño. However, Figure 15 indicates that the water in the tropics was colder than normal indicating, if anything, the presence of an "anti-El Niño." A plausible explana-
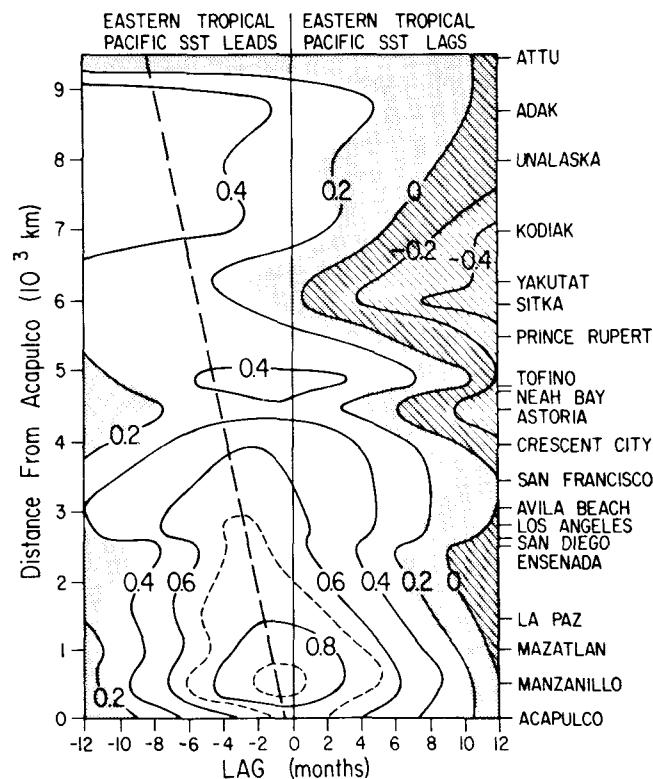

Figure 16. Contour plot of the correlation between low-frequency (13-month running mean) SLH in month t at each of the 20 tide gauge stations and low-frequency eastern tropical Pacific SST in month (t + lag). Shaded region corresponds to artificial correlation expected purely by chance from sampling errors, and cross hatching indicates negative correlations. Dashed straight line is meant to aid the eye in locating the approximate region of maximum correlation and corresponds to approximately 50 cm/sec northward propagation.
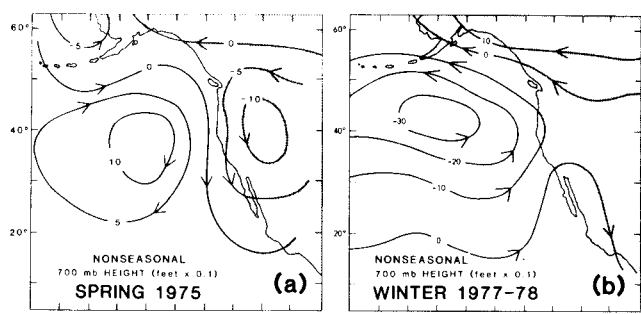
Figure 17. Contour plots of nonseasonal 700 mb height for a) spring of 1975 and, b) winter of 1977-78. Arrows indicate direction of nonseasonal upper air flow.

tion for the discrepancy can be found from an examination of meteorological records over the eastern Pacific. The anomalous 700 mb height taken from Namias (1979) for winter 1977-78 is shown in Figure 17b. The arrows indicate the direction of anomalous air flow in the upper atmosphere. There was a very large-scale air flow from the south which was responsible for the 1978 heavy rainfall in southern California (more than twice the normal value). These basin-wide winds would be expected to drive an anomalous poleward flow as observed during 1978. Recall from Figure 5 that the salinity behaved differently during 1978 than was anticipated from the advective model. The anomalous poleward flow would produce the observed increase in temperature at 50-m depth shown in Figure 5b by advection. However, an increase in salinity would also be anticipated but Figure 5c shows that in fact the salinity at 50 m decreased during 1978.

Figure 18 shows the time development of the vertical structure of temperature and salinity along Cal-COFI line 93 during the winter of 1977-78. The temperature field for December of 1977 shows an increase nearshore and a decrease farther offshore. A maximum temperature anomaly of about 1°C occurred at a depth of about 100m which, as can be seen from Figure 7, corresponds to the depth of the permanent thermocline. This suggests that tilting of the isotherms was responsible for the temperature anomalies. During January and February of 1978 this anomalous temperature signal became better developed with warm water nearshore throughout the water column and anomalously cold water farther offshore throughout the water column. Again, the region of maximum anomaly is located at about the depth of the permanent thermocline reflecting the tilting of isotherms associated with geostrophic adjustment of the pycnocline to anomalous poleward flow. That is, with poleward flow, the isotherms nearshore tilt downward while those farther offshore rise toward the surface.

The salinity field cannot be explained in the same manner. In December of 1977 the salinity was near

normal. There is the hint of a tongue of low salinity water offshore at station 80 (unfortunately stations 90 and 100 were not occupied during December of 1977). By January and February of 1978 the low salinity anomaly was fully developed. A maximum of $-0.4\%o$ occurred near the surface at the farthest offshore stations.

The combination of warm, low-salinity water near the surface cannot be explained by a local rearrangement of any of the water masses typically present in this region. It must be concluded that some new water was somehow introduced to the region. The heavy rainfall during winter 1977-78 would reduce the salinity of the surface waters but would not be expected to have much of an effect below the thermocline. However, Figure 18 shows that, although most of the decrease is concentrated near the surface, the anomalously low salinity extended throughout the water column. The magnitude of the anomaly at 500 m was around 0.02-$0.04\%o$ during February of 1978. An estimate of the amount of excess freshwater from precipitation required to produce the observed anomalous salinity can be made by ignoring effects of advection and assuming that all mixing occurred locally. Then, the total amount of salt in the water column remains fixed so that

$$\iiint_{\text{Volume}} S \, dV = \text{Constant}$$

and the excess freshwater that must be added to an initial column of water of depth D_M and salinity S_M to produce an anomalous salinity S_A is given by

$$\Delta D = D_M \left(\frac{S_M}{S_A} - 1 \right).$$

The integrated effects of the observed anomalous salinity for February of 1978 from the mean February salinity distribution for the upper 500 m along line 93 are shown in Figure 19. Although the distribution of rainfall over the ocean is not well understood, the values shown in Figure 19 seem too high when compared with the precipitation values recorded at the coast. The excess rainfall in southern California amounted to about 0.5 m for the entire rainy season (late November through May). Figure 19 indicates that about 0.5 m of excess rainfall would be required prior to February to account for the observed salinity anomaly nearshore and about 1-2 m of excess rainfall would be required at the offshore stations. It is also difficult to explain how this freshwater could be mixed to depths of 500 m. So, although the high precipitation off southern California certainly contributed to the winter 1977-78 salinity anomaly near the surface, it cannot account for all of the necessary excess fresh-
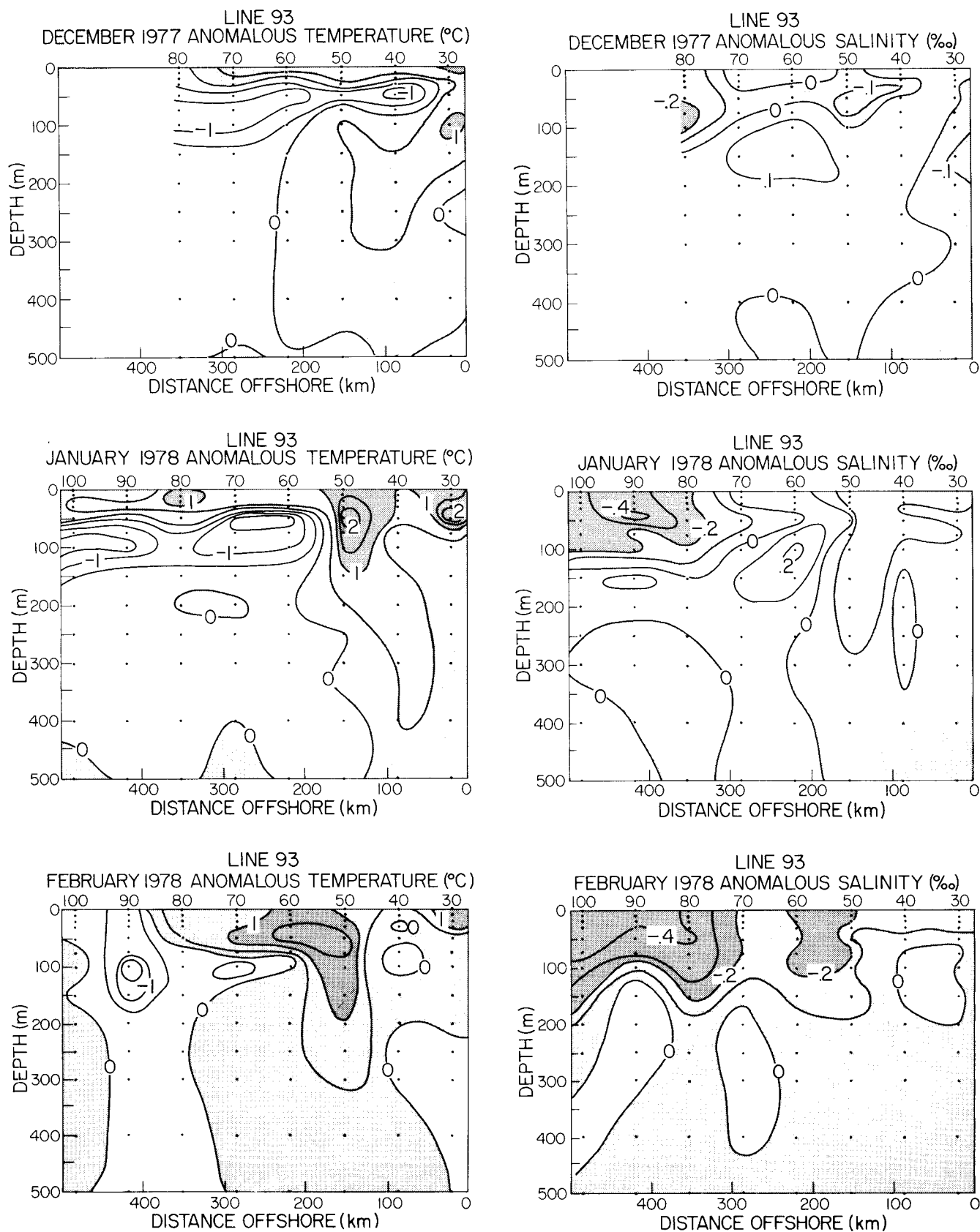
Figure 18. Anomalous temperature and salinity along CalCOFI line 93 for the months of December of 1977 and January and February of 1978. The CalCOFI station number is shown along the top of each plot. Positive temperature anomalies and negative salinity anomalies are shaded in the figures.
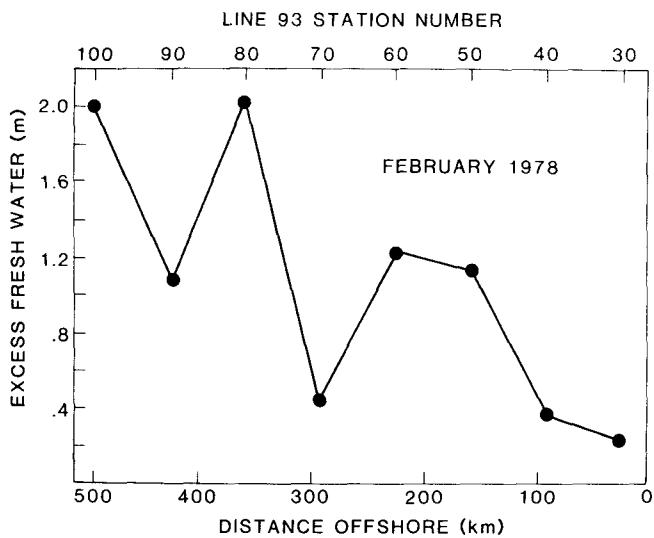
LINE 93 STATION NUMBER

Figure 19. Excess freshwater required to explain the anomalous salinity of a column of water at each station along CalCOFI line 93 for the month of February 1978.

water. There must have been horizontal movement of freshwater into the region off southern California from some other region.

The source of this freshwater remains a mystery at the present time. Two plausible explanations can be proposed. The first is that the freshwater may have originated off the northwest coast of the United States from excess rainfall during the preceding summer. With a southward velocity of 20 cm/sec, water off the coast of Washington would reach San Diego 4-5 months later.

A second possible explanation is suggested by the large-scale wind pattern shown in Figure 17b. The southerly winds would drive an onshore Ekman transport, resulting in broad-scale downwelling conditions. This could produce the thin layer of warm water present near the surface everywhere during December of 1977 and January of 1978. And if the salinity was below normal in the offshore waters, it could also produce the observed salinity anomalies.

Unfortunately, the three-year sampling pattern subsequent to 1969 and the limited geographical extent of the CalCOFI program preclude the possibility of testing either of these hypotheses. Data from 1977 and data farther offshore are needed to look at the time evolution of the temperature and salinity fields leading up to the winter of 1977-78. The expendable bathythermograph (XBT) and surface salinity data collected from merchant ships by the National Marine Fisheries Service between San Francisco and Honolulu may shed some light on the processes leading to the 1977-78 winter conditions in the California Current.

It is worth pointing out that the temperature and salinity conditions in the California Current during 1975 are the reverse of those found in 1978. Figure 5d shows that the southward transport was higher than normal, so anomalously low temperatures and salinities would be anticipated. Figures 5b and 5c show that the 50-m temperature was about 0.5 degree below normal as expected but the salinity was about 0.1%oo higher than normal. Figure 17a shows that anomalous atmospheric conditions during spring 1975 were also the reverse of those found in winter 1977-78, with large-scale northerly air flow off the coast of California. This suggests that there might be a connection between the atmospheric and oceanic conditions and the physical processes responsible for both anomalies. This discussion has been purely qualitative based on case studies from only two events and is certainly worthy of more detailed study. But it does point out the lack of a complete understanding of all of the large-scale processes in the California Current. A quantitative index of the large-scale aspects of atmospheric forcing in a time series sense would allow a statistical comparison between this broad-scale wind forcing and the biological and physical oceanography of the California Current.

SUMMARY

In summary, it has been demonstrated here that increased zooplankton volume is associated with a decrease in water temperature. The two potential sources of this cold water (upwelling and advection) produce opposing effects on the salinity distribution; advection of high-nutrient water from high latitudes would decrease the salinity, whereas upwelling of deeper high-nutrient water would result in an increase in salinity. Local coastal upwelling appears to be poorly related statistically to the zooplankton variability. It is concluded that large-scale advection plays the dominant role in controlling zooplankton biomass in the California Current. These large-scale variations are significantly related to El Niño occurrences in the eastern tropical Pacific and can be conveniently monitored from coastal tide gauge records along the California Coast.

A great deal of attention was drawn to the anomalous conditions in the California Current during 1978. Temperature and salinity anomalies generally tend to be of the same sign. That is, anomalously cold water generally tends to be low in salinity, reflecting higher latitude origin. Similarly, anomalously warm water generally tends to be high in salinity, reflecting low-latitude origin. However, during 1978 the water in the California Current was unusually warm but low in salinity. It was shown that anomalous rainfall during

the same time period cannot account for all of the salinity anomaly. It was suggested that the excess freshwater required to produce the observed salinity anomaly must have been transported horizontally into the region either by downstream advection or by on-shore Ekman transport driven by anomalous wind forcing. Similar but opposite conditions existed during 1975: anomalously cool water was high in salinity.

An important result of this study is that it points out some limitations in the present three-year CalCOFI sampling pattern. In particular, the three-year spacing is not adequate to determine the physical processes responsible for the anomalous events of 1975 and 1978. It also points out that, although the dominant patterns of physical and biological variability have been drawn out in this analysis, there are still other important large-scale processes occurring that are not yet understood.

ACKNOWLEDGMENTS

LITERATURE CITED

Bernal, P. A. 1979: Large-scale biological events in the California Current. Calif. Coop. Oceanic Fish. Invest. Rep. 20: 89-101.

Bernal, P. A. 1980: Large-scale biological events in the California Current: The low frequency response of the epipelagic ecosystem. PhD dissertation, Scripps Institution of Oceanography, University of California San Diego, 184 p.

Bernal, P. A., and J. A. McGowan. 1981. Advection and upwelling in the California Current. To be published in the proceedings of the CUEA symposium.

Caton, F. G., M. J. Cuming, and B. R. Mendenhall. 1978. A northern hemisphere history of marine wind-based parameters. Meteorology International Inc., Tech. Rep. M-231, 106 p.

Chelton, D. B. 1980. Low frequency sea level variability along the west coast of North America. PhD dissertation, Scripps Institution of Oceanography, University of California, San Diego, 212 p.

Colebrook, J. M. 1977. Annual fluctuations in biomass of taxonomic groups of zooplankton in the California Current, 1955-59. Fish. Bull., U.S. 75: 357-368.

Davis, R. E. 1976. Predictability of sea surface temperature and sea level pressure anomalies over the North Pacific Ocean. J. Phys. Oceanog. 6: 249-266.

McCreary, J. P. 1976. Eastern tropical ocean response to changing wind systems: with application to El Niño. J. Phys. Oceanog. 6:632-645.

Namias, J. 1979. Northern hemisphere seasonal 700mb height and anomaly charts, 1947-1978, and associated North Pacific sea surface temperature anomalies. Calif. Coop. Oceanic Fish. Invest. Atlas 27, 275 p.

Nelson, C. S. 1977. Wind stress and wind stress curl over the California Current. NOAA Tech. Rep. NMFS SSRF-714, August 1977.

Reid, J. L., G. L. Roden, and J. G. Wyllie. 1958. Studies in the California Current System. Calif. Coop. Oceanic Fish. Invest. Rep. 5:28-57.

Soutar, A. 1971. Micropaleontology of anaerobic sediments and the California Current. In B. M. Funnell and W. R. Reidel (eds.), The Micropaleontology of Oceans. Cambridge University Press, Cambridge, p. 223-230.

Wickett, W. P. 1967. Ekman transport and zooplankton concentration in the North Pacific Ocean. J. Fish. Res. Board Can. 24:581-594.